COMPUTER METHODS IN APPLIED MECHANICS AND ENGINEERING 59 (1986) 155–177
NORTH-HOLLAND

STREAM FUNCTION AND STREAM-FUNCTION-COORDINATE (SFC) FORMULATION FOR INVISCID FLOW FIELD CALCULATIONS

Chung-Yuan HUANG and George S. DULIKRAVICH*

Texas Institute for Computational Mechanics (TICOM), Department of Aerospace Engineering and Engineering Mechanics, The University of Texas at Austin, Austin, TX, U.S.A.

Received 23 August 1985
Revised manuscript received 10 February 1986

Three-dimensional, steady, inviscid, compressible, isoenergetic, rotational flows can be completely described by two families of stream functions. In the present study, explicit forms of the governing equations for these two stream functions of baratropic fluid flows are derived. With the assumptions of two-dimensional or axisymmetric, incompressible and/or irrotational flows, this formulation can be reduced to the familiar special cases.

The concept of stream-function-coordinate (SFC) is introduced along with some relevant examples. Exact gas dynamic equations using stream functions as independent variables are also presented. Applications and difficulties involved with the SFC concept are clearly exposed, and several possible ways to resolve these problems are discussed.

1. Introduction

The velocity potential function and stream functions are commonly employed to reduce the number of unknowns in the calculation of fluid flow problems. Both approaches suffer the penalty of increasing the order of the original governing partial differential equations. Furthermore, the introduction of a velocity potential function is based on the assumption of an irrotational flow. However, the stream function formulation is suitable for rotational flow calculations.

The earliest work involving a stream function formulation can be traced back to 1781, when Lagrange [1] introduced the stream function for two-dimensional planar incompressible flows. The stream function for incompressible axisymmetric flows was found by Stokes [2] in 1842. Yih [3] pointed out that both methods used to find the stream functions are based on strictly mathematical considerations without any connection to flow kinematics. It was in 1951 that Giese [4] proposed that steady, inviscid, three-dimensional, rotational flows can be described by two families of stream functions. By properly choosing the formulation for the second stream function, Giese proved that the stream functions introduced by Lagrange and Stokes are only special cases of the first stream function that he defined.

The physical meaning [4] of these two families of stream functions is that each of the two stream functions corresponds to a family of stream surfaces. The intersection contour of these two stream surfaces represents a streamline. The mass flux through a stream tube bounded by two pairs of stream surfaces can be expressed as the product of the differences of these two

*Present address: Aerospace Engineering Department, Pennsylvania State University, University Park, PA 16802, U.S.A.

stream functions. Giese also verified a variational principle for three-dimensional steady compressible flows by using the concept of two stream functions.

In 1957, Yih [3] mathematically proved the existence of two stream functions for three-dimensional steady flows by means of flow kinematics and verified the results obtained by Giese. Moreover, Yih extended his mathematical approach to unsteady flows and concluded that for three-dimensional unsteady compressible flows three separate path functions exist. Each of these three path functions corresponds to a family of material surfaces. Velocity components and the mass contained in a material volume bounded by three material surfaces can be expressed in terms of the three path functions. Since the vorticity vector belongs to a solenoidal vector field, and since the equation of a vortex line is analogous to the equation of a stream line, Yih asserted that two vorticity functions can be applied equally well to describe the vortex motion.

Even though Giese and Yih applied different approaches to find stream functions for three-dimensional flows, they did not provide any examples to emphasize their mathematical results. In 1963, Benton [5], following Yih's idea, mathematically designed a potential flow consisting of a single three-dimensional quadrupole with two orthogonal axes and found the explicit form for two stream functions describing such a flow.

It should be pointed out that the assumption of an incompressible flow mathematically uncouples the energy equation from both the continuity and momentum equations. In addition, if the flow is assumed to be irrotational, the equation of continuity also becomes uncoupled from the momentum equations, and the velocity field can be completely determined solely by using flow kinematics. One of the objectives of this study is to combine flow kinematics and flow dynamics to find the governing equations of two stream functions describing three-dimensional, steady, inviscid, compressible, isoenergetic, and rotational flows.

The second objective is to introduce the stream-function-coordinate (SFC) formulation for the purpose of solving a flow problem and simultaneously determining the flow pattern. Basically, this concept represents a transformation of the stream function equations in such a way that stream functions ψ and λ are treated as new independent variables, while y- and z-coordinates are treated as new dependent variables. Since the body profile corresponds to a stream surface (or a streamline in planar two-dimensional cases), boundary conditions for the transformed equation become very simple and numerical methods can be readily applied to solve this equation.

It is worth noting that this concept can be applied to both incompressible [6] and compressible [7–10] flows. The third and most important objective of this paper is to clearly expose several essential problems involved with the SFC concept and with the use of stream functions in general for fluid flow computations. Possible ways to resolve some of these difficulties will also be discussed.

2. Exact stream function formulation

The momentum equations for steady, inviscid flows without body forces can be written in vector operator form as

$$\rho[\nabla \tfrac{1}{2} V \cdot V - V \times \nabla \times V] = -\nabla p \,, \tag{1}$$

where p is the local thermodynamic pressure, and V is the local fluid velocity vector. The nondimensional mass flux vector u is defined as

$$u = \rho V/\rho^* a^* , \tag{2}$$

where ρ^*, a^* denote the critical density and critical speed of sound, respectively, and they are constant for isoenergetic flows. Let us define two scalar functions ψ and λ in such a way that

$$u = \nabla\psi \times \nabla\lambda . \tag{3}$$

It is seen that the equation of continuity in the absence of mass sources and sinks,

$$\nabla \cdot u = \nabla\lambda \cdot (\nabla \times \nabla\psi) - \nabla\psi \cdot (\nabla \times \nabla\lambda) \equiv 0 , \tag{4}$$

is identically satisfied using this formulation. This is the celebrated Clebsch transformation, which is cited in [21, 22] and has been applied with increasing frequency in recent years [23–27], particularly in connection with studies of secondary flow in turbomachinery.

The vorticity vector ω can be rewritten in terms of the nondimensional mass flux vector u as

$$\omega = \nabla \times V = \rho^* a^* [(\nabla \times u)/\rho + \nabla(1/\rho) \times u] . \tag{5}$$

Hence

$$\nabla \times u + u \times \nabla\rho/\rho = \rho\omega/\rho^* a^* . \tag{6}$$

For baratropic fluid flows, pressure is a function of density only, i.e.,

$$p = p(\rho) . \tag{7}$$

The local speed of sound is defined as

$$a^2 = (\partial p/\partial \rho)_s . \tag{8}$$

Thus, the momentum equation (1) can be expressed in terms of nondimensional mass flux u as

$$\tfrac{1}{2}(\rho^* a^*)^2 \nabla(u \cdot u/\rho^2) - \rho^* a^* u \times \omega/\rho = -\nabla p/\rho = -(a^2/\rho)\nabla\rho . \tag{9}$$

Let us define a compressibility parameter k by

$$k^2 = (\rho^* a^*/\rho a)^2 . \tag{10}$$

Then, (9) reduces to

$$-k^2 u \cdot u \nabla\rho/\rho + k^2 \nabla(\tfrac{1}{2} u \cdot u) - k u \times \omega/a = -\nabla\rho/\rho . \tag{11}$$

Hence,

$$\nabla\rho/\rho = \frac{k^2\nabla(\frac{1}{2}\boldsymbol{u}\cdot\boldsymbol{u}) - k\boldsymbol{u}\times\boldsymbol{\omega}/a}{k^2\boldsymbol{u}\cdot\boldsymbol{u}-1}\,. \tag{12}$$

Replacing $\nabla\rho/\rho$ in (6) by equation (12), we have

$$\nabla\times\boldsymbol{u} + \frac{k^2\boldsymbol{u}\times\nabla(\frac{1}{2}\boldsymbol{u}\cdot\boldsymbol{u})}{k^2\boldsymbol{u}\cdot\boldsymbol{u}-1} = \frac{-\boldsymbol{\omega} + k^2\boldsymbol{u}(\boldsymbol{\omega}\cdot\boldsymbol{u})}{ka(k^2\boldsymbol{u}\cdot\boldsymbol{u}-1)}\,. \tag{13}$$

Substituting (3) into equation (11) results in

$$\nabla\times(\nabla\psi\times\nabla\lambda) + \frac{k^2(\nabla\psi\times\nabla\lambda)\times\nabla[\frac{1}{2}(\nabla\psi\times\nabla\lambda)\cdot(\nabla\psi\times\nabla\lambda)]}{k^2(\nabla\psi\times\nabla\lambda)\cdot(\nabla\psi\times\nabla\lambda)-1}$$
$$= \frac{-\boldsymbol{\omega} + k^2(\nabla\psi\times\nabla\lambda)[\boldsymbol{\omega}\cdot(\nabla\psi\times\nabla\lambda)]}{ka[k^2(\nabla\psi\times\nabla\lambda)\cdot(\nabla\psi\times\nabla\lambda)-1]}\,. \tag{14}$$

Note that (14) represents the explicit vector operator form of the flow governing equations involving the stream function equations for three-dimensional, steady, inviscid, isoenergetic, rotational flows. Since $\boldsymbol{\omega} = \nabla\times\boldsymbol{V}$ and hence $\nabla\cdot\boldsymbol{\omega} = 0$, (14) actually represents two independent coupled scalar equations. Any two equations resulting from (14) can be used to solve for ψ and λ.

For irrotational flows, (14) reduces to

$$\nabla\times(\nabla\psi\times\nabla\lambda) + \frac{k^2(\nabla\psi\times\nabla\lambda)\times\nabla[\frac{1}{2}(\nabla\psi\times\nabla\lambda)\cdot(\nabla\psi\times\nabla\lambda)]}{k^2[(\nabla\psi\times\nabla\lambda)\cdot(\nabla\psi\times\nabla\lambda)]-1} = 0\,. \tag{15}$$

Crocco's theorem states that steady, homoenergetic, and irrotational flow must also be homentropic. Thus, the compressibility parameter k can be written as

$$k^2 = (\rho^*a^*/\rho a)^2 = [\tfrac{1}{2}(\gamma+1) - \tfrac{1}{2}(\gamma-1)M^{*2}]^{-(\gamma+1)/(\gamma-1)}\,, \tag{16}$$

where $M^* = |V|/a^*$ is the characteristic or critical local Mach number. For two-dimensional planar flows, the second stream function is $\lambda = z$. Then, (14) becomes

$$(1-k^2\psi_y^2)\psi_{xx} + 2k^2\psi_x\psi_y\psi_{xy} + (1-k^2\psi_x^2)\psi_{yy} = \omega[k^2(\psi_x^2+\psi_y^2)-1]/ka\,. \tag{17}$$

For two-dimensional irrotational flows, (14) becomes

$$(1-k^2\psi_y^2)\psi_{xx} + 2k^2\psi_x\psi_y\psi_{xy} + (1-k^2\psi_x^2)\psi_{yy} = 0\,. \tag{18}$$

For two-dimensional incompressible flows $k = 0$ and (14) reduces to

$$\psi_{xx} + \psi_{yy} = -\omega\,. \tag{19}$$

For two-dimensional incompressible, irrotational flows $k = 0$ and $\omega = 0$, and (14) reduces to

$$\psi_{xx} + \psi_{yy} = 0 . \tag{20}$$

The complete forms of flow governing equations using the stream function formulation written in terms of polar and cylindrical coordinates are given in Appendix A.

The best known application of the two-dimensional form of (14) in the precomputer era is summarized in the research reports of Emmons [11–13]. He solved the stream function equation for two-dimensional transonic flows by hand relaxation in which the shock was fitted. In recent years, different versions of the transonic stream function equations for two-dimensional and three-dimensional flows have been studied. Chin and Rizzeta [14] obtained the small-perturbation version of the two-dimensional stream function equation that is deduced from the transonic small-perturbation potential equation. They successfully applied it to airfoil inverse design in subcritical and supercritical flows.

Since the conservative form of the two-dimensional stream function equation is very similar to the potential equation, Hafez [15] and Lovell [16] applied the artificial compressibility method, that has often been used for potential flow problems, to solve the transonic stream function equation in conservation form for both irrotational and rotational flows. Their computational results showed that inviscid separation is possible with the stream function formulation for rotational transonic flows. The first successful numerical calculation of three-dimensional transonic flows using two stream functions was performed by Sherif and Hafez [17]. However, the two stream functions that they used to calculate three-dimensional flows do not represent physical stream surfaces. Instead, they represent two components of a generalized vector potential.

Since the stream function formulation is suitable for rotational flow problems, Atkins and Hassan [18] considered the rotational effects due to the generation of vorticity behind a shock wave. By applying the stream function formulation to the Euler equations of gas dynamics, they were able to avoid explicit evaluation of the vorticity. They concluded that numerical solutions of the Euler equations based on stream function formulations are accurate and relatively inexpensive.

3. Stream-function-coordinate (SFC) concept

In recent years, the streamline and stream-function-coordinate (SFC) concept has been applied in numerical calculations of several elementary flow problems. Table 1 summarizes recent publications related to these applications. Among those, it should be pointed out that only Pearson [9] formulated the problem for three-dimensional flows and only Breeze-Stringfellow and Burggraf [6] worked with the physical stream function (axisymmetric incompressible flows) and obtained the explicit form of the transformed equation.

In this section, the exact transformations of the three-dimensional stream function equations will be derived [19]. It was mentioned earlier that two stream functions in three-dimensional flows correspond to two families of stream surfaces. However, the body surface in a flow field is a stream surface. Thus, the use of stream function coordinates will transform the body surface from the physical domain into a strip (or line segment for two-dimensional flows) in the transformed domain. It should be noted that the boundary conditions for the transformed equations are highly simplified, thus numerical methods can be readily applied to solve the

Table 1
Summary of recent publications utilizing SFC formulation

Researchers	Applied coordinate systems	Formulation of governing equations	Applications
R. Ishii 1980 [7, 8]	Streamline α and orthogonal trajectory of streamline β	1. Continuity equation 2. Irrotationality 3. Energy equation 4. Equation of state 5. Kinematic relations	Subsonic and supersonic axially symmetric nozzle flow calculations
C.E. Pearson 1981 [9]	x, α and β; α and β are any two parameters that can be used to identify different streamlines	1. Continuity equation 2. Momentum equations 3. Energy equation 4. Equation of state 5. Kinematic relations	Subsonic jet flow with free surface
A.K. Singhal and D.B. Spalding 1983 [10]	x and stream function ψ (two-dimensional flows)	1. Continuity equation 2. Momentum equations 3. Equation of state 4. Kinematic relations	Subsonic and transonic flows in a cascade of turbine blade
A.Breeze-Stringfellow and O.R. Burggraf 1983 [6]	x and stream function ψ (incompressible axisymmetric flows)	1. Continuity equation (Incompressible flow) 2. Irrotationality	Propeller and nacelle interference

transformed equations. Several example calculations are presented to demonstrate the applications.

Equation (14) contains combinations of first-order and second-order partial derivatives for both ψ and λ. Thus, only the transformations for the first-order and the second-order partial derivatives are needed.

For simplicity, we will consider a Cartesian coordinate system only. The transformations using any other coordinate system can be obtained by a similar procedure. The old dependent variables in the full stream function equations are

$$\psi = \psi(x, y, z), \qquad \lambda = \lambda(x, y, z). \tag{21}$$

The new dependent variables are

$$x = x(x, \psi, \lambda), \qquad y = y(x, \psi, \lambda), \qquad z = z(x, \psi, \lambda). \tag{22}$$

We first assume that the functions x, y, and z are continuously differentiable with respect to the new independent variables x, ψ, and λ. Define

$$[J] = \begin{bmatrix} x_x & x_\psi & x_\lambda \\ y_x & y_\psi & y_\lambda \\ z_x & z_\psi & z_\lambda \end{bmatrix} \tag{23}$$

as the Jacobian matrix of the transformation given by (22). Then

$$J_1 = \det[J] = y_\psi z_\lambda - y_\lambda z_\psi \tag{24}$$

is the determinant of the Jacobian matrix.

The transformation of the first-order partial derivatives can be obtained from the inverse of the Jacobian matrix as

$$[J]^{-1} = [A]^{\mathrm{t}}/J_1 ,$$

where $[A]^{\mathrm{t}}$ denotes the adjoint matrix of $[J]$. The elements in matrix $[A]$ are equal to the cofactors of the corresponding elements in matrix $[J]$. Therefore, the inverse of the Jacobian matrix can be expressed as

$$\begin{bmatrix} x_x & x_y & x_z \\ \psi_x & \psi_y & \psi_z \\ \lambda_x & \lambda_y & \lambda_z \end{bmatrix} = \frac{1}{J_1} \begin{bmatrix} J_1 & 0 & 0 \\ J_2 & z_\lambda & -y_\lambda \\ J_3 & -z_\psi & y_\psi \end{bmatrix} , \tag{25}$$

where

$$J_1 = y_\psi z_\lambda - y_\lambda z_\psi , \qquad J_2 = y_\lambda z_x - y_x z_\lambda , \qquad J_3 = y_x z_\psi - y_\psi z_x . \tag{26}$$

The partial derivative of the identity matrix with respect to x gives that

$$([J][J]^{-1})_x = ([I])_x = 0 . \tag{27}$$

After rearranging, it follows that

$$\begin{bmatrix} x_{xx} & x_{xy} & x_{xz} \\ \psi_{xx} & \psi_{xy} & \psi_{xz} \\ \lambda_{xx} & \lambda_{xy} & \lambda_{xz} \end{bmatrix} = -[J]^{-1} \begin{bmatrix} (x_x)_x & (x_\psi)_x & (x_\lambda)_x \\ (y_x)_x & (y_\psi)_x & (y_\lambda)_x \\ (z_x)_x & (z_\psi)_x & (z_\lambda)_x \end{bmatrix} [J]^{-1} = -[J]^{-1}[F][J]^{-1} , \tag{28}$$

where $[F]$ denotes the matrix involving mixed derivatives of new variables and old variables. The elements of $[F]$ can be determined by chain rule differentiation as follows:

$$\begin{aligned}
&(x_x)_x = (x_\psi)_x = (x_\lambda)_x = 0 , \\
&(y_x)_x = x_x y_{xx} + \psi_x y_{x\psi} + \lambda_x y_{x\lambda} = y_{xx} + (J_2/J_1) y_{x\psi} + (J_3/J_1) y_{x\lambda} , \\
&(y_\psi)_x = x_x y_{\psi x} + \psi_x y_{\psi\psi} + \lambda_x y_{\psi\lambda} = y_{x\psi} + (J_2/J_1) y_{\psi\psi} + (J_3/J_1) y_{\psi\lambda} , \\
&(y_\lambda)_x = x_x y_{\lambda x} + \psi_x y_{\lambda\psi} + \lambda_x y_{\lambda\lambda} = y_{x\lambda} + (J_2/J_1) y_{\psi\lambda} + (J_3/J_1) y_{\lambda\lambda} , \\
&(z_x)_x = x_x z_{xx} + \psi_x z_{x\psi} + \lambda_x z_{x\lambda} = z_{xx} + (J_2/J_1) z_{x\psi} + (J_3/J_1) z_{x\lambda} , \\
&(z_\psi)_x = x_x z_{\psi x} + \psi_x z_{\psi\psi} + \lambda_x z_{\psi\lambda} = z_{x\psi} + (J_2/J_1) z_{\psi\psi} + (J_3/J_1) z_{\psi\lambda} , \\
&(z_\lambda)_x = x_x z_{\lambda x} + \psi_x z_{\lambda\psi} + \lambda_x z_{\lambda\lambda} = z_{x\lambda} + (J_2/J_1) z_{\psi\lambda} + (J_3/J_1) z_{\lambda\lambda} .
\end{aligned} \tag{29}$$

Therefore, (28) becomes

$$\begin{bmatrix} 0 & 0 & 0 \\ \psi_{xx} & \psi_{xy} & \psi_{xz} \\ \lambda_{xx} & \lambda_{xy} & \lambda_{xz} \end{bmatrix} = -[A]^t[F][A]^t/J_1^2 . \tag{30}$$

Similarly, by taking the partial derivative of the identity matrix with respect to y and z, we get

$$\begin{bmatrix} 0 & 0 & 0 \\ \psi_{yx} & \psi_{yy} & \psi_{yz} \\ \lambda_{yx} & \lambda_{yy} & \lambda_{yz} \end{bmatrix} = -[A]^t[G][A]^t/J_1^2 \tag{31}$$

and

$$\begin{bmatrix} 0 & 0 & 0 \\ \psi_{zx} & \psi_{zy} & \psi_{zz} \\ \lambda_{zx} & \lambda_{zy} & \lambda_{zz} \end{bmatrix} = -[A]^t[H][A]^t/J_1^2 , \tag{32}$$

where the matrices $[G]$ and $[H]$ are similar to $[F]$ as follows:

$$[G] = \begin{bmatrix} (x_x)_y & (x_\psi)_y & (x_\lambda)_y \\ (y_x)_y & (y_\psi)_y & (y_\lambda)_y \\ (z_x)_y & (z_\psi)_y & (z_\lambda)_y \end{bmatrix} , \tag{33}$$

$$[H] = \begin{bmatrix} (x_x)_z & (x_\psi)_z & (x_\lambda)_z \\ (y_x)_z & (y_\psi)_z & (y_\lambda)_z \\ (z_x)_z & (z_\psi)_z & (z_\lambda)_z \end{bmatrix} . \tag{34}$$

The elements in matrices $[G]$ and $[H]$ can be determined by the same method that was used to determine matrix $[F]$. The results are

$$\begin{gathered} (x_x)_y = (x_\psi)_y = (x_\lambda)_y = (x_x)_z = (x_\psi)_z = (x_\lambda)_z = 0 , \\ (y_x)_y = \frac{z_\lambda}{J_1} y_{x\psi} - \frac{z_\psi}{J_1} y_{x\lambda} , \qquad (z_x)_y = \frac{z_\lambda}{J_1} z_{x\psi} - \frac{z_\psi}{J_1} z_{x\lambda} , \\ (y_\psi)_y = \frac{z_\lambda}{J_1} y_{\psi\psi} - \frac{z_\psi}{J_1} y_{\psi\lambda} , \qquad (z_\psi)_y = \frac{z_\lambda}{J_1} y_{\psi\psi} - \frac{z_\psi}{J_1} z_{\psi\lambda} , \\ (y_\lambda)_y = \frac{z_\lambda}{J_1} y_{\psi\lambda} - \frac{z_\psi}{J_1} y_{\lambda\lambda} , \qquad (z_\lambda)_y = \frac{z_\lambda}{J_1} y_{\psi\lambda} - \frac{z_\psi}{J_1} y_{\lambda\lambda} , \end{gathered} \tag{35}$$

$$\begin{gathered} (y_x)_z = -\frac{y_\lambda}{J_1} y_{x\psi} + \frac{y_\psi}{J_1} y_{x\lambda} , \qquad (z_x)_z = -\frac{y_\lambda}{J_1} z_{x\psi} + \frac{y_\psi}{J_1} z_{x\lambda} , \\ (y_\psi)_z = -\frac{y_\lambda}{J_1} y_{\psi\psi} + \frac{y_\psi}{J_1} y_{\psi\lambda} , \qquad (z_\psi)_z = -\frac{y_\lambda}{J_1} z_{\psi\psi} + \frac{y_\psi}{J_1} z_{\psi\lambda} , \\ (y_\lambda)_z = -\frac{y_\lambda}{J_1} y_{\psi\lambda} + \frac{y_\psi}{J_1} y_{\lambda\lambda} , \qquad (z_\lambda)_z = -\frac{y_\lambda}{J_1} z_{\psi\lambda} + \frac{y_\psi}{J_1} z_{\lambda\lambda} . \end{gathered} \tag{36}$$

4. SFC formulation for two-dimensional flows

For two-dimensional planar flows, $\lambda = z$ and it follows that

$$\psi_x = J_2/J_1 = -y_x/y_\psi , \qquad \psi_y = z_\lambda/J_1 = 1/y_\psi . \tag{37}$$

The second-order partial derivatives ψ_{xx}, ψ_{xy}, and ψ_{yy} can be determined from (30) and (31). The results are

$$\psi_{xx} = (-1/y_\psi^3)(y_x^2 y_{\psi\psi} - 2y_x y_\psi y_{x\psi} + y_\psi^2 y_{xx}) , \tag{38}$$

$$\psi_{xy} = (1/y_\psi^3)(y_x y_{\psi\psi} - y_\psi y_{x\psi}) , \tag{39}$$

$$\psi_{yy} = -y_{\psi\psi}/y_\psi^3 . \tag{40}$$

Substituting (38)–(40) into equations (17)–(20), the SFC equations for different types of flow are obtained.

For two-dimensional rotational compressible planar flows:

$$(y_\psi^2 - k^2)y_{xx} - 2y_x y_\psi y_{x\psi} + (1 + y_x^2)y_{\psi\psi} = -\omega[k^2(1 + y_x^2)y_\psi - y_\psi^3]/ka . \tag{41}$$

For two-dimensional irrotational compressible planar flows:

$$(y_\psi^2 - k^2)y_{xx} - 2y_x y_\psi y_{x\psi} + (1 + y_x^2)y_{\psi\psi} = 0 . \tag{42}$$

For two-dimensional rotational incompressible planar flows:

$$y_\psi^2 y_{xx} - 2y_x y_\psi y_{x\psi} + (1 + y_x^2)y_{\psi\psi} = \omega y_\psi^3 . \tag{43}$$

For two-dimensional irrotational incompressible planar flows:

$$y_\psi^2 y_{xx} - 2y_x y_\psi y_{x\psi} + (1 + y_x^2)y_{xx} = 0 . \tag{44}$$

Nevertheless, at the points where the Jacobian vanishes or tends to infinity the transformation is not unique. The Jacobian of the transformation is given by (24) as

$$J_1 = y_\psi z_\lambda - y_\lambda z_\psi . \tag{45}$$

This expression provides no information about the location of those singular points. However, (25) gives that

$$y_\psi = J_1\lambda_z , \qquad z_\lambda = J_1\psi_y , \qquad y_\lambda = -J_1\psi_z , \qquad z_\psi = -J_1\lambda_y . \tag{46}$$

Substituting into (24), it follows that

$$J_1 = 1/(\psi_y\lambda_z - \psi_z\lambda_y) = 1/V_x . \tag{47}$$

From (47) we can immediately conclude that the transformation fails at the points where the x-component of the velocity vector equals zero or infinity. This means that the location of singular points implicitly depends on the solution of the velocity field and explicitly on the geometry of the boundaries of the flow domain.

In order to analyze the significance of this problem, a number of numerical computations were performed, and the results were compared with analytic solutions. Problems arising from the applications of the SFC concept are demonstrated by three examples of two-dimensional flows:

(a) Steady, uniform incompressible flow through a cascade of doublets. The exact form [20] of the stream function for this flow is given as

$$\psi = U_\infty\left[y - [(2H/\pi)\sinh^2(\pi c/4H)]\,\frac{\sin(\pi y/H)}{\cosh(\pi x/H) - \cos(\pi y/H)}\right], \tag{48}$$

where c is the chord length of the resulting oval shaped body in the cascade, and $2H$ is the distance between the centers of the ovals. In this particular example, $c = 1.8366$ and $H = 2.0$ were used.

(b) Steady incompressible potential flow around a corner. The exact form of the stream function for this flow problem is

$$\psi = U_\infty R^n \sin(n\theta) . \tag{49}$$

(c) Compressible subsonic steady potential flow around a NACA 0012 airfoil in a channel. The equation to be solved is the stream-function-coordinate equation:

$$(Y_\psi^2 - K^2)Y_{xx} - 2Y_x Y_\psi Y_{x\psi} + (1 + Y_x^2)Y_{\psi\psi} = 0 , \tag{50}$$

where $K = 0$ for incompressible flow problems. From the discriminant of this equation,

$$D = Y_\psi^2(M^2 - 1) , \tag{51}$$

Table 2
Computational efficiency

Examples	Convergence criteria	Grid size	Execution time on CDC 170/750
Incompressible potential flow through a cascade of doublets	$\delta_{max} = 10^{-5}$	91 × 11	6 s for uniform mesh 12 s for nonuniform mesh
Incompressible potential corner flow	$\delta_{max} = 10^{-5}$	65 × 11	4 s
Subsonic flow around NACA 0012 airfoil in a channel with height/chord = 3.6	$\delta_{max} = 10^{-5}$	91 × 11	10 s for $M_\infty = 0.01$ 44 s for $M_\infty = 0.65$

we can immediately conclude that the type of the original stream function equation is preserved in both compressible and incompressible flow situations.

Numerical discretization of the governing SFC equations was performed using central differences to formulate the finite difference equations. Let subscripts i and j denote the ith node along the x-axis and the j-th streamline, respectively, then the following finite difference forms are obtained:

$$Y_x = \frac{Y_{i+1,j} - Y_{i-1,j}}{(\Delta x_i + \Delta x_{i-1})} = A , \tag{52}$$

$$Y_\psi = \frac{Y_{i,j+1} - Y_{i,j-1}}{(\Delta \psi_j + \Delta \psi_{j-1})} = B , \tag{53}$$

$$Y_{xx} = \frac{2[Y_{i+1,j}\,\Delta x_{i-1} - Y_{i,j}(\Delta x_i + \Delta x_{i-1}) + Y_{i-1,j}\,\Delta x_i]}{\Delta x_i\,\Delta x_{i-1}(\Delta x_i + \Delta x_{i-1})} , \tag{54}$$

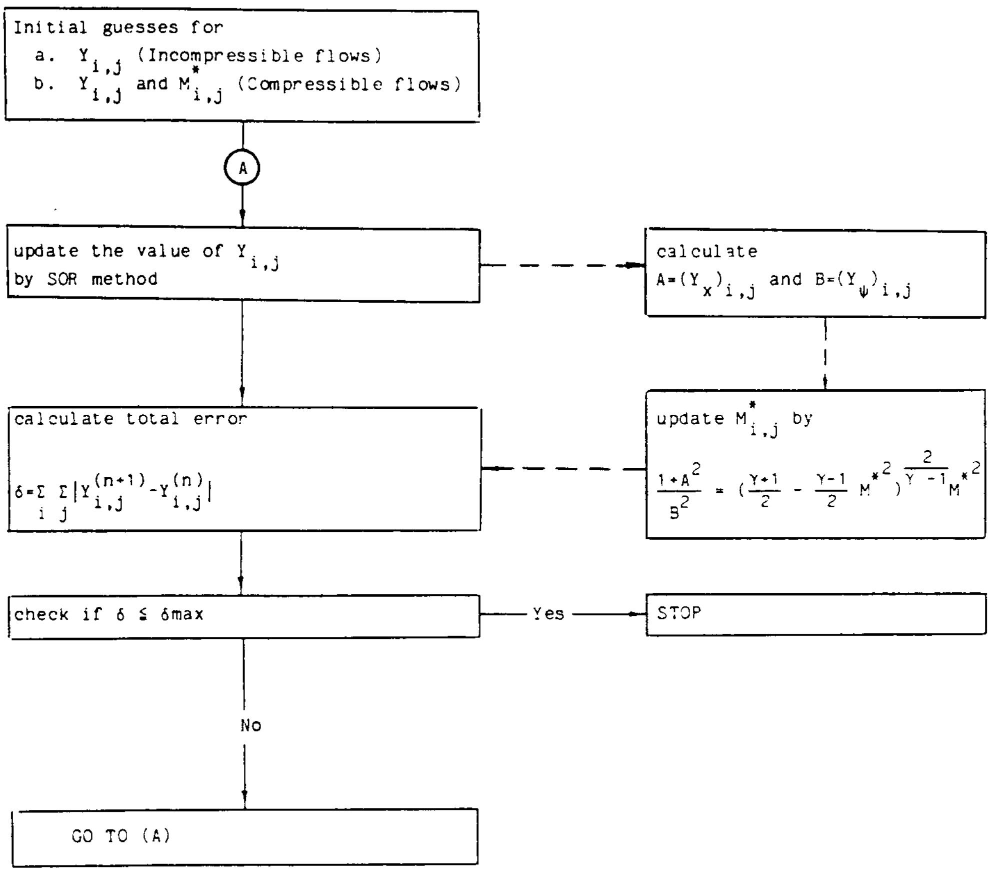

Fig. 1. Iterative algorithm flow chart.

$$Y_{\psi\psi} = \frac{2[Y_{i,j+1}\,\Delta\psi_{j-1} - Y_{i,j}(\Delta\psi_j + \Delta\psi_{j-1}) + Y_{i,j-1}\,\Delta\psi_j]}{\Delta\psi_j\,\Delta\psi_{j-1}(\Delta\psi_j + \Delta\psi_{j-1})}\,, \tag{55}$$

$$Y_{x\psi} = \frac{Y_{i-1,j+1} - (Y_{i-1,j-1} + Y_{i-1,j+1}) + Y_{i-1,j-1}}{(\Delta x_i + \Delta x_{i-1})(\Delta\psi_j + \Delta\psi_{j-1})} = C\,, \tag{56}$$

where, in general, $\Delta f_i = f_{i+1} - f_i$. Substituting (52)–(56) into equation (50) and rearranging the terms, we obtain the finite difference equation for steady potential flows

$$Y_{i,j} = \left[\frac{(B^2 - K^2)}{\Delta x_i\,\Delta x_{i-1}} + \frac{(1 + A^2)}{\Delta\psi_j\,\Delta\psi_{j-1}}\right]^{-1}\left[\frac{(B^2 - K^2)(Y_{i+1,j}\,\Delta x_{i-1} + Y_{i-1,j}\,\Delta x_i)}{\Delta x_i\,\Delta x_{i-1}(\Delta x_i + \Delta x_{i-1})} + \frac{(1 + A^2)(Y_{i,j+1}\,\Delta\psi_{j-1} + Y_{i,j-1}\,\Delta\psi_j)}{\Delta\psi_j\,\Delta\psi_{j-1}(\Delta\psi_j + \Delta\psi_{j-1})} - ABC\right]. \tag{57}$$

Equation (57) was solved iteratively using the method of successive overrelaxations.

The iterative algorithm flow chart is schematically represented in Fig. 1, where the dashed lines indicate the steps used for compressible flow computations.

5. Numerical results

Figures 2–5 show the numerical results and the normalized error distribution for a uniform incompressible steady flow past a cascade of doublets. As was mentioned earlier, the analytic transformation used in the SFC formulation fails at the points where the x-component of the velocity vector equals zero. This results in a locally large numerical error. The error distribution also shows that this error is localized in the region near the singular point. Several

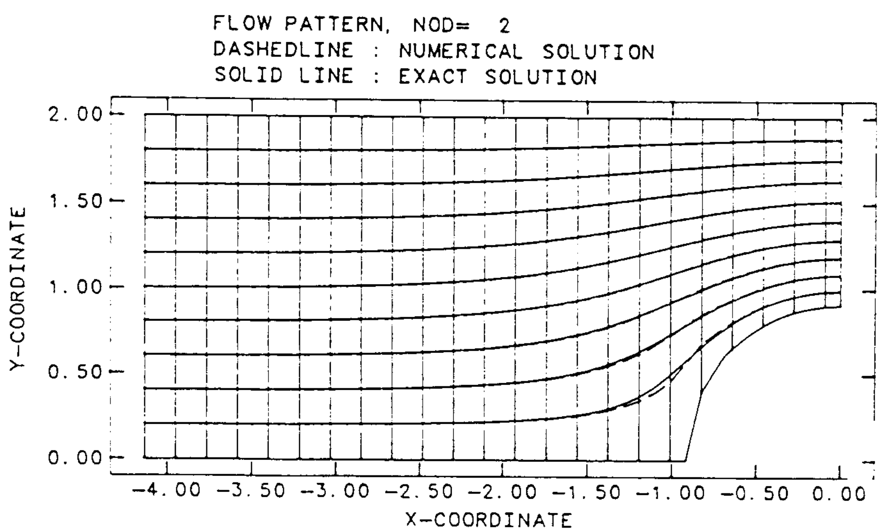

Fig. 2. Exact and numerical solutions of a uniform flow through a cascade of doublets: Uniform grid.

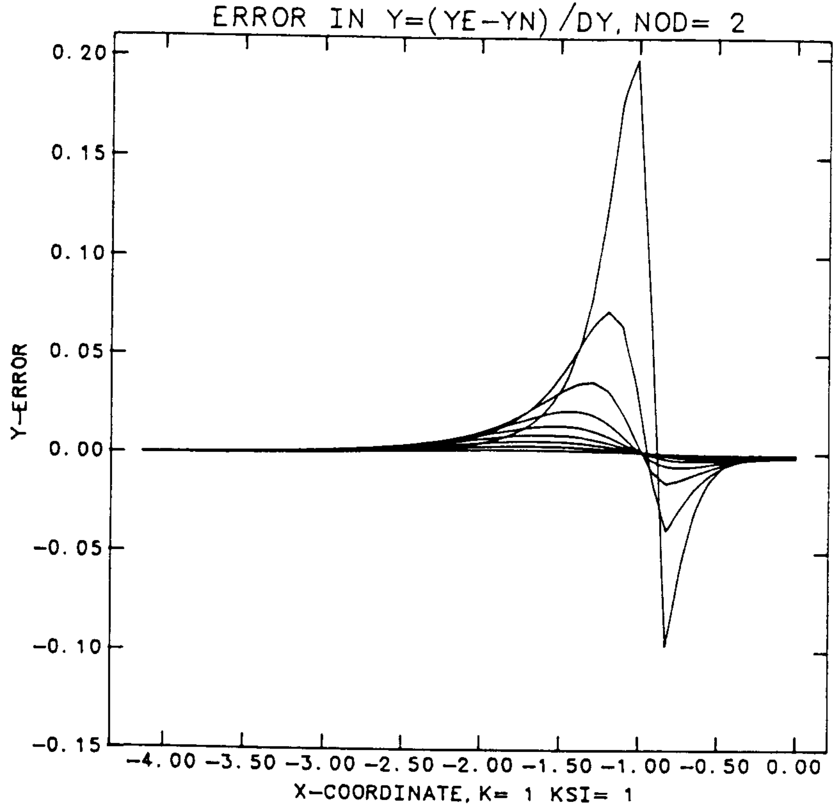

Fig. 3. Normalized error distribution: Uniform grid.

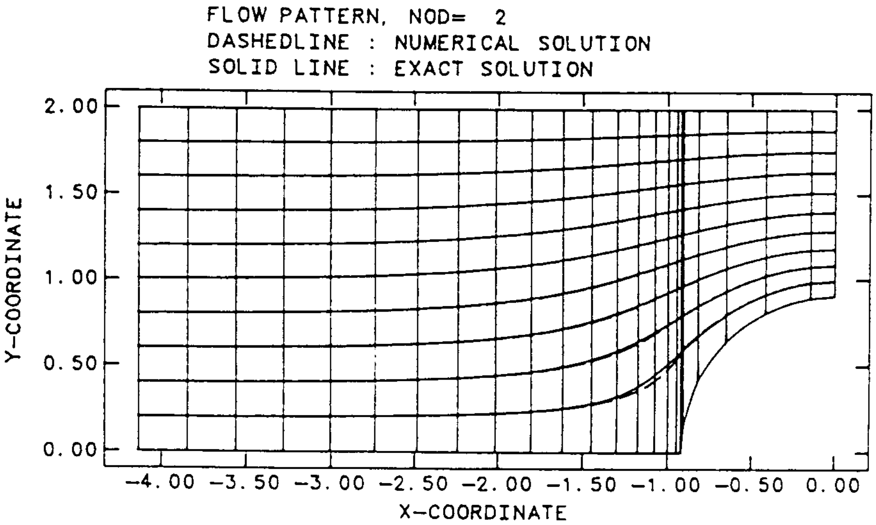

Fig. 4. Exact and numerical solutions of a uniform flow through a cascade of doublets: Nonuniform grid.

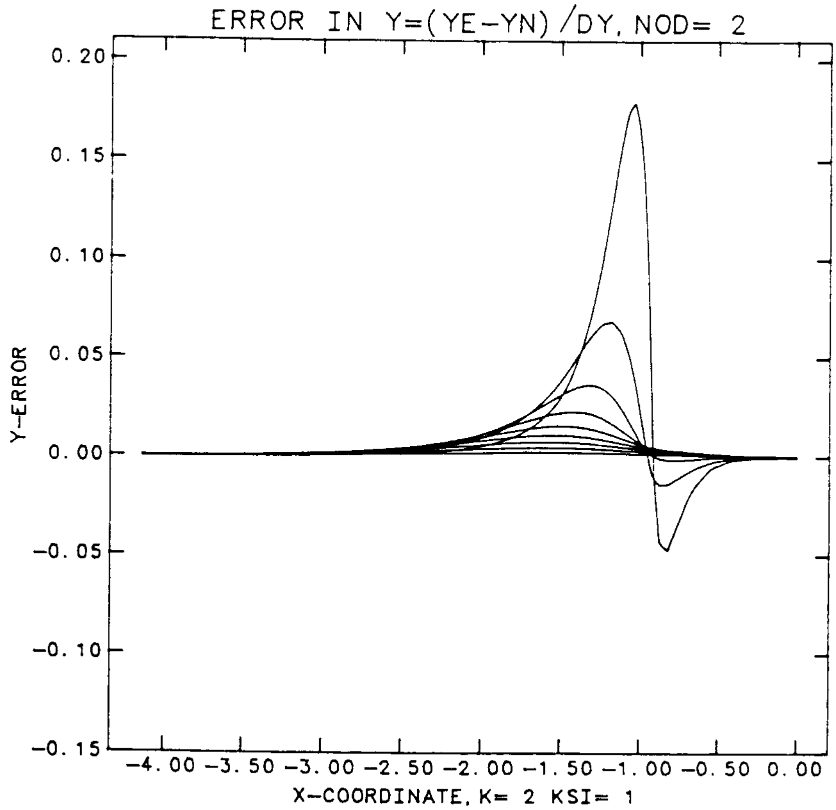

Fig. 5. Normalized error distribution: Nonuniform grid.

different strategies for clustering of the grid about the singular point were attempted. However, the error persisted as shown in Fig. 5.

Figures 6 and 7 show that, in the case of a uniform flow past a concave corner, the numerical error is significantly reduced with the decrease of the angle of the corner. It should be pointed out that numerical solutions for the shape of streamlines are usually so close to the analytic solutions that this visual effect often misleads one to believe that the computations are correct. High-accuracy results could be expected only if a body has a cusped leading edge with the cusp centerline perfectly aligned with a streamline. Nevertheless, the streamline shapes are not known a priori, and the appropriate shapes and locations of the cusp cannot be specified in advance.

In the case of steady uniform subsonic flow around a NACA 0012 airfoil, a number of numerical tests with varying free-stream Mach numbers were studied. The calculated pressure coefficients on the surface of the airfoil agree well with the data from other numerical methods, as shown in Fig. 8. Nevertheless, local numerical errors at the leading edge and at the trailing edge stagnation points are noticeable.

In the derivation of the SFC equations based on the Cartesian coordinate system, it was demonstrated that singular points occurred wherever the x-component of the velocity vector vanishes or becomes infinite. Recent publications [6, 9, 10] related to the applications of the

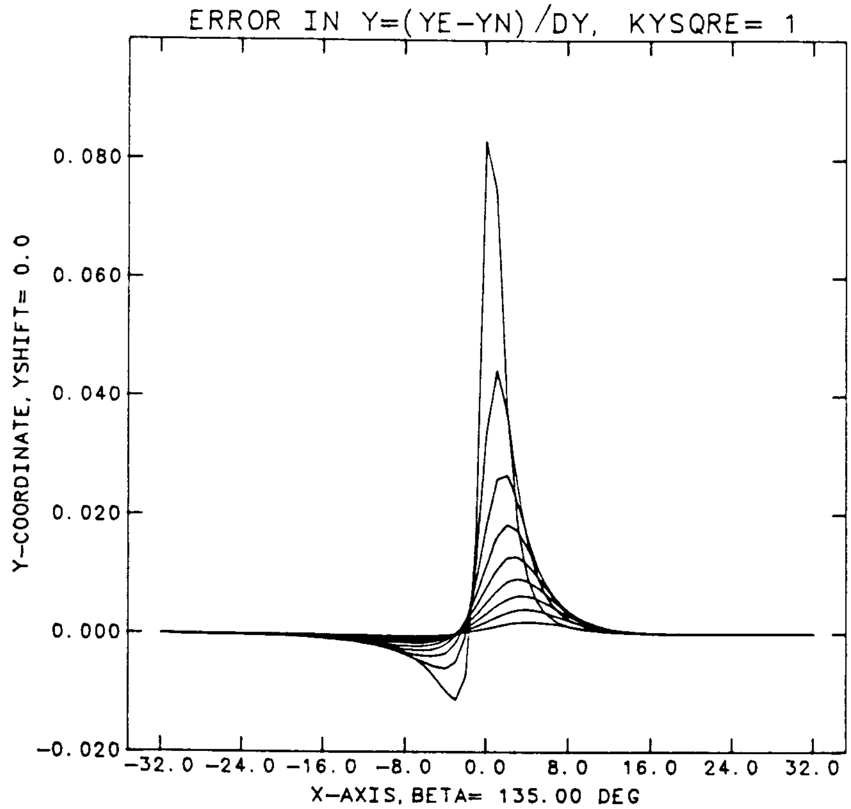

Fig. 6. Normalized error distribution for the corner flow with $\beta = 135°$.

SFC concept do not stress the fact that these singular points of transformation implicitly depend not only on the solution of the velocity field, but explicitly depend on the geometry of the boundary as well. Hence, the locations of all singular points are not known a priori and cannot be treated a priori.

The Jacobian in Pearson's formulation [9] does not have an obvious physical meaning. However, Pearson pointed out that the x-coordinate may be considered as a convenient independent variable only when the streamlines are nowhere perpendicular to the x-axis, which severely limits the practical applicability of the method.

Breeze-Stringfellow and Burggraf [6] suggested the use of a finer grid in the region near the singular point in order to improve the accuracy. Our numerical results show that large local numerical errors persist even when using a finely clustered grid near the stagnation point. Since the stagnation point is a true singular point of the transformation, local grid clustering is not capable of removing this analytic singularity.

Singhal and Spalding [10] used a rather approximate method of placing a small cusp at the stagnation point to remove this problem. Nevertheless, the orientation, size, and actual location of the cusp cannot be specified a priori if the correctness of the solution is not to be severely compromised.

There are several other essential problems related to this technique. Since the Y-coordinate

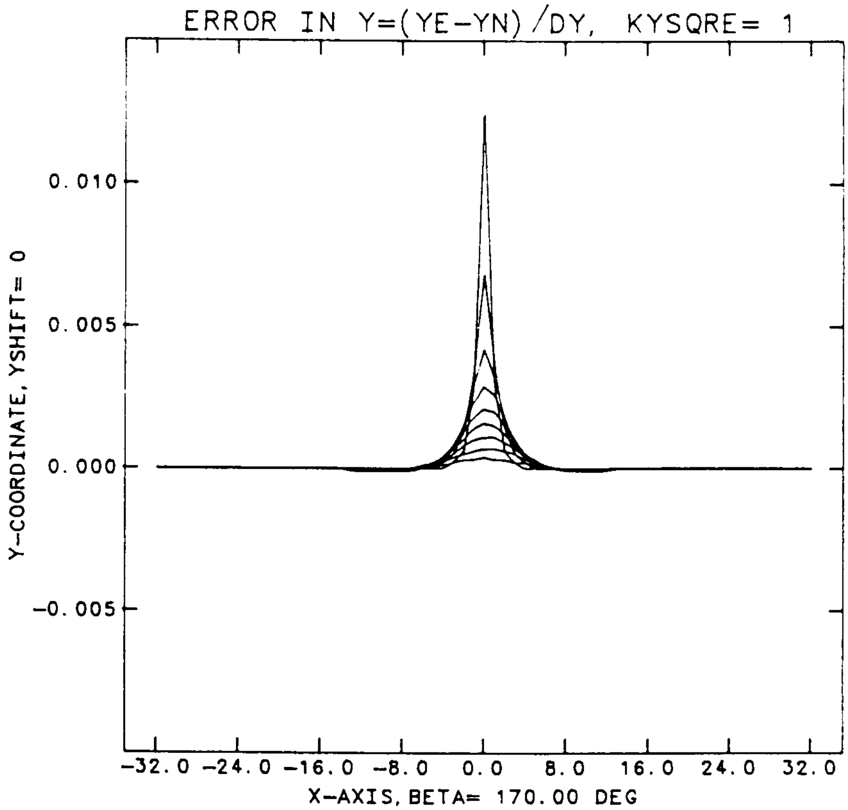

Fig. 7. Normalized error distribution for the corner flow with $\beta = 170°$.

is treated as a new dependent variable in the SFC equation, multiple-valuedness problems could arise. For a uniform flow at moderate angles of attack, Y is double-valued on the dividing streamline, as sketched in Fig. 9. For a uniform flow with higher angle of attack, Y is triple-valued on the streamlines that are very close to the body, as sketched in Fig. 10. In the case of a triple-valued problem, it is important to note that points A and B are singular points of transformation although the velocities are not zero there. This means that the numerically obtained results at points A and B will be unacceptably inaccurate.

One attempt was made to resolve the issue of double-valued problems. A new dependent variable $\bar{Y}$ was defined as

$$\bar{Y} = [Y - Y_c(x)]^2 , \tag{58}$$

$$Y_c(x) = \tfrac{1}{2}(Y_U(x) + Y_L(x)) . \tag{59}$$

Here, $Y_U(x)$, $Y_L(x)$, and $Y_c(x)$ represent the equations for upper, lower, and camber surfaces of the airfoil, respectively. With the new dependent variable $\bar{Y}$, the surface of the body is transformed into a curved plate of zero thickness. The governing equation for this new dependent variable $\bar{Y}$ is

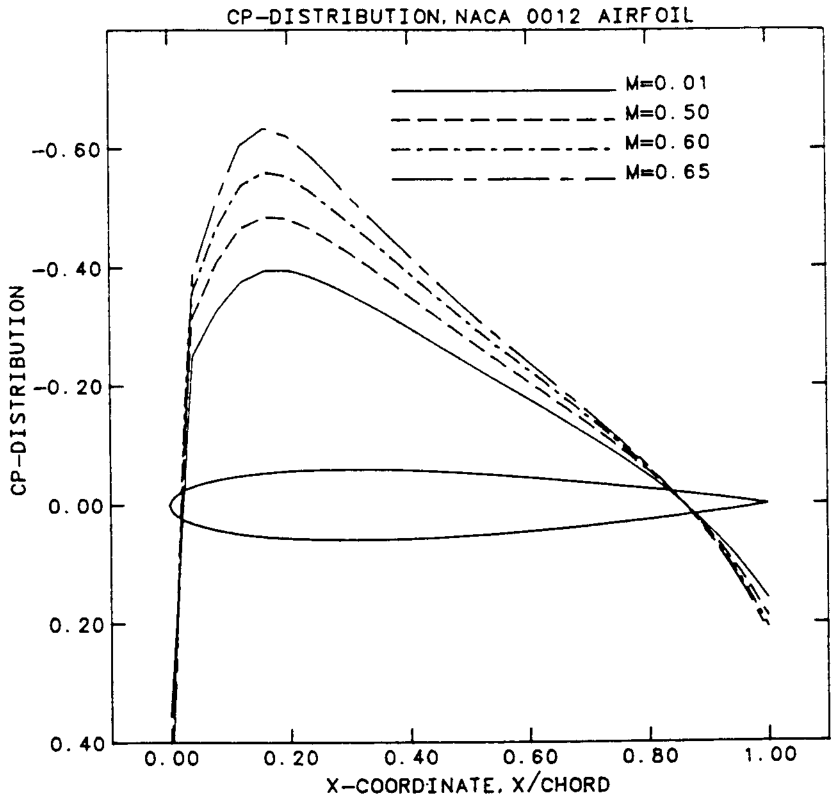

Fig. 8. Computed pressure distribution for the NACA 0012 airfoil at different Mach numbers.

$$(\bar{Y}_\psi^2 - K^2)\bar{Y}_{xx} - 2\bar{Y}_x Y_\psi \bar{Y}_{x\psi} + (4\bar{Y} + \bar{Y}_x^2)\bar{Y}_{\psi\psi} = 2\bar{Y}_\psi^2 , \tag{60}$$

with $K = 0$ for incompressible flows.

A uniform incompressible potential flow around a corner with several different values of $Y_c(x)$ was used to test this idea. Results are shown in Figs. 11–13. The conclusion is that the accuracy strongly depends on the choice of $Y_c(x)$. This is probably due to the new singularities that are introduced with this new transformation. Indeed, the Jacobian of the new transformation

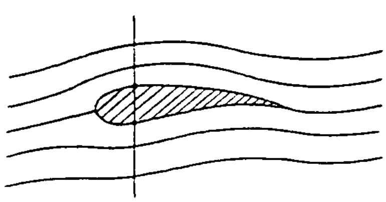

Fig. 9. Double-valued problem.

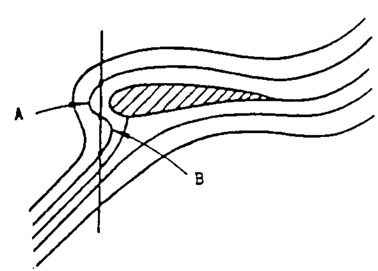

Fig. 10. Triple-valued problem.

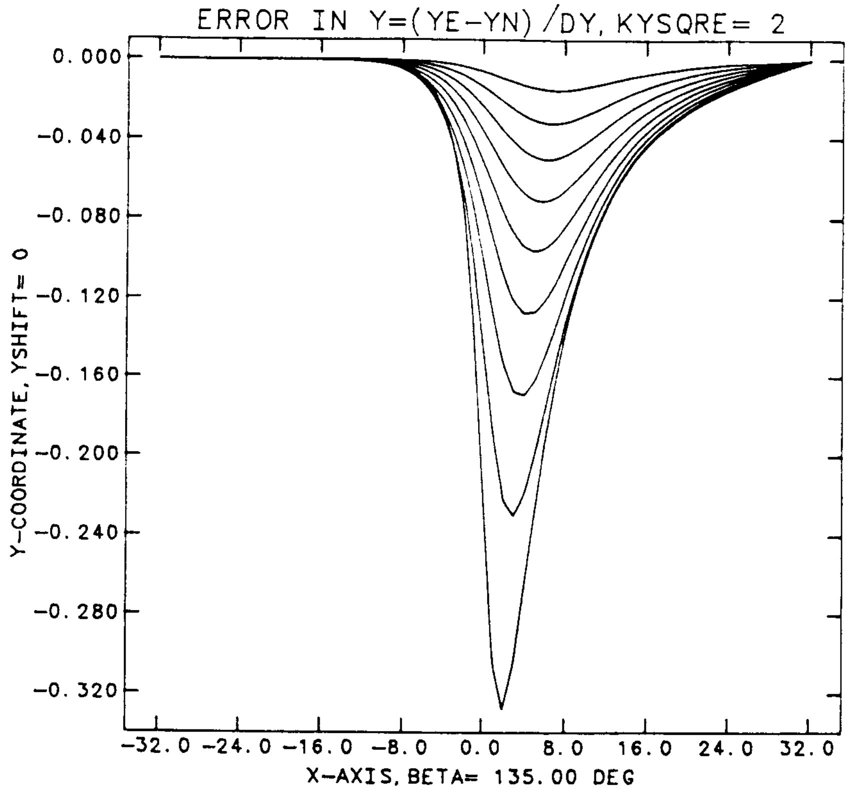

Fig. 11. Normalized error distribution, $\beta = 135°$, $Y_c = 0$.

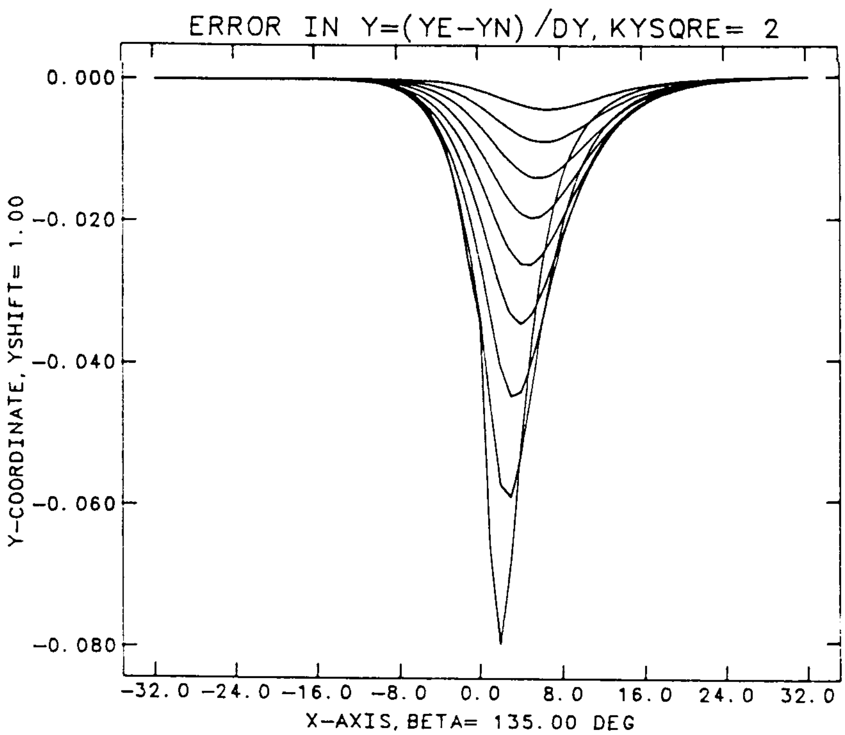

Fig. 12. Normalized error distribution, $\beta = 135°$, $Y_c = 1.0$.

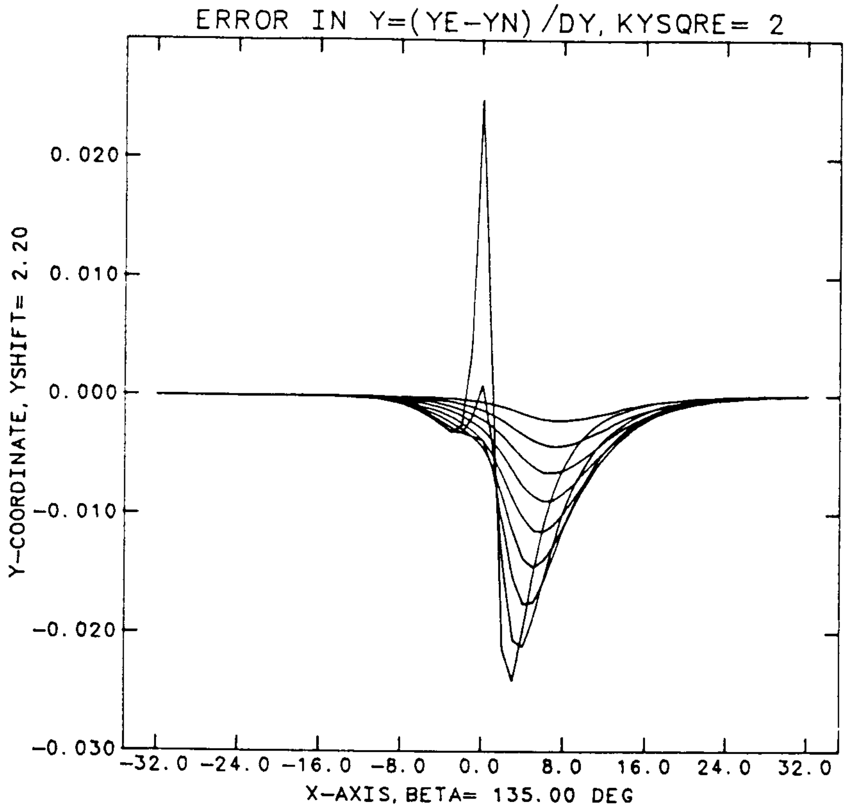

Fig. 13. Normalized error distribution, $\beta = 135°$, $Y_c = 2.2$.

$$J = \bar{Y}_\psi = 2[Y - Y_c(x)]Y_\psi = 2[Y - Y_c(x)]/V_x \tag{61}$$

shows that $Y = Y_c(x)$ represents a line of singularity, part of which is hidden inside the original body.

6. Conclusions

Explicit vector operator forms of the three-dimensional stream function equations and the transformed equations based on the SFC concept were derived. A number of example calculations of both incompressible and compressible flow problems were carried out by using the transformed stream function equations. The essential problems involved with this concept and the possible ways to resolve these problems were discussed.

The significant features of this concept are summarized as follows:

(a) The formulation is always conservative.

(b) Boundary conditions are highly simplified. Thus, this concept is suitable for solving inviscid flow problems with complex boundaries.

(c) This method is applicable to both incompressible and compressible flow problems.

(d) Only a one-dimensional grid (x-coordinate or θ-coordinate) is required for solving two-dimensional problems. The other family of grid lines, representing streamlines, is automatically generated as a part of the solution.

(e) Singular points of the transformation are dependent not only on the geometry of the boundary, but also implicitly on the solution of the velocity field. If numerical errors caused by the singular points of the transformation could be efficiently reduced, this method could be used for solving both direct and inverse problems of inviscid fluid dynamics.

(f) Singular points of the transformation are the sources of large local numerical errors in the regions close to the singular points.

(g) Multiple-valued results represent possible problems accompanying the transformed stream function equations. Nevertheless, this is a disadvantage of any formulation involving stream functions, thus precluding their application for the calculation of recirculating separated flows.

Appendix A

A.1. Stream function equations in polar coordinates ($\lambda = z$)

Full equation:

$$[1 - (k\psi_\theta^2/r)]\psi_{,rr} + (2k^2\psi_{,r}\psi_{,\theta}/r^2)\psi_{,r\theta} + [1 - (k\psi_{,r})^2]\psi_{,\theta\theta}/r^2 + (\psi_{,r}/r)[1 - (k\psi_{,r})^2 - 2(k\psi_{,\theta}/r)^2] = \omega[(k\psi_{,\theta}/r)^2 + (k\psi_{,r})^2 - 1]/ka\,. \quad \text{(A.1)}$$

For irrotational flows, (A.1) becomes

$$[1 - (k\psi_{,\theta}/r)^2]\psi_{,rr} + (2k^2\psi_{,r}\psi_{,\theta}/r^2)\psi_{,r\theta} + [1 - (k\psi_{,r})^2]\psi_{,\theta\theta}/r^2 + (\psi_{,r}/r)[1 - (k\psi_{,r})^2 - 2(k\psi_{,\theta}/r)^2] = 0 \quad \text{(A.2)}$$

For incompressible flows, (A.1) becomes

$$\psi_{,rr} + \psi_{,\theta\theta}/r^2 + \psi_{,r}/r = -\omega\,. \quad \text{(A.3)}$$

For incompressible, irrotational flows, (A.1) becomes

$$r^2\psi_{,rr} + \psi_{,\theta\theta} + r\psi_{,r} = 0\,. \quad \text{(A.4)}$$

A.2. Stream function equations in cylindrical coordinates ($\lambda = \theta$)

Full equation:

$$[1 - (k\psi_{,z}/r)^2]\psi_{,rr} + 2k^2(\psi_{,r}\psi_{,z}/r^2)\psi_{,rz} + [1 - (k\psi_{,r}/r)^2]\psi_{,zz} - \psi_{,r}/r = \omega r[k^2/r^2(\psi_{,r}^2 + \psi_{,z}^2) - 1]/ka\,. \quad \text{(A.5)}$$

For irrotational flows, (A.5) becomes

$$[1 - (k\psi_{,z}/r)^2]\psi_{,rr} + 2k^2(\psi_{,r}\psi_{,z}/r^2)\psi_{,rz} + [1 - (k\psi_{,r}/r)^2]\psi_{,zz} - \psi_{,r}/r = 0\,. \quad \text{(A.6)}$$

For incompressible flows, (A.5) becomes

$$\psi_{rr} + \psi_{zz} - \psi_r/r = -r\omega \ . \tag{A.7}$$

For incompressible and irrotational flows, (A.5) reduces to

$$\psi_{rr} + \psi_{zz} - \psi_r/r = 0 \ . \tag{A.8}$$

A.3. Stream-function-coordinate equations in polar coordinates ($\lambda = z$)

Full equation:

$$\begin{aligned}(r^2 + r_\theta^2)r_{\psi\psi} - 2r_\theta r_\psi r_{\theta\psi} + (r_\psi^2 - k^2)r_{\theta\theta} + r[2(kr_\theta/r)^2 + k^2 - r_\psi^2] \\ = \omega r_\psi[r^2 r_\psi^2 - k^2(r_\theta^2 + r^2)]/ka \ .\end{aligned} \tag{A.9}$$

For irrotational flows, (A.9) becomes

$$(r^2 + r_\theta^2)r_{\psi\psi} - 2r_\theta r_\psi r_{\theta\psi} + (r_\psi^2 - k^2)r_{\theta\theta} + r[2(kr_\theta/r)^2 + k^2 - r_\psi^2] = 0 \ . \tag{A.10}$$

For incompressible flows, (A.9) becomes

$$(r^2 + r_\theta^2)r_{\psi\psi} - 2r_\theta r_\psi r_{\theta\psi} + r_\psi^2 r_{\theta\theta} - rr_\psi^2 = \omega r^2 r_\psi^3 \ . \tag{A.11}$$

For incompressible irrotational flows, (A.9) becomes

$$(r^2 + r_\theta^2)r_{\psi\psi} - 2r_\theta r_\psi r_{\theta\psi} + r_\psi^2 r_{\theta\theta} - rr_\psi^2 = 0 \ . \tag{A.12}$$

A.4. Stream-function-coordinate equations in cylindrical coordinates ($\lambda = \theta$)

Full equation:

$$(1 + r_z^2)r_{\psi\psi} - 2r_\psi r_z r_{\psi z} + (r_\psi^2 - k^2/r^2)r_{zz} + r_\psi^2/r = \omega r r_\psi(r_\psi^2 - k^2/r^2 - k^2 r_z^2/r^2)/ka \ . \tag{A.13}$$

For irrotational flows, (A.13) becomes

$$(1 + r_z^2)r_{\psi\psi} - 2r_\psi r_z r_{\psi z} + (r_\psi^2 - k^2/r^2)r_{zz} + r_\psi^2/r = 0 \ . \tag{A.14}$$

For incompressible flows, (A.13) becomes

$$(1 + r_z^2)r_{\psi\psi} - 2r_\psi r_z r_{\psi z} + r_\psi^2 r_{zz} + r_\psi^2/r = \omega r r_\psi^3 \ . \tag{A.15}$$

For incompressible, irrotational flows, (A.13) becomes

$$(1 + r_z^2)r_{\psi\psi} - 2r_\psi r_z r_{\psi z} + r_\psi^2 r_{zz} + r_\psi^2/r = 0 \ . \tag{A.16}$$

A.5. Jacobians of the transformations in various coordinate systems

In Cartesian coordinates, $\psi(x, y) \rightarrow y(x, \psi)$,

$$J = \det\begin{bmatrix} x_x & x_\psi \\ y_x & y_\psi \end{bmatrix} = y_\psi = 1/\psi_y = 1/V_x . \tag{A.17}$$

The transformation fails at all points where the x-components of the local velocity vector equal zero or infinity.

In polar coordinates, $\psi(r, \theta) \rightarrow r(\psi, \theta)$,

$$J = \det\begin{bmatrix} r_\theta & r_\psi \\ \theta_\theta & \theta_\psi \end{bmatrix} = -r\psi = -1/\psi_r = 1/V_\theta . \tag{A.18}$$

The transformation fails at all points where the θ-component of the local velocity vector equals zero or infinity.

In cylindrical coordinates, $\psi(r, z) \rightarrow r(\psi, z)$,

$$J = \det\begin{bmatrix} r_z & r_\psi \\ z_z & z_\psi \end{bmatrix} = -r_\psi = -1/\psi_r = -1/rV_z . \tag{A.19}$$

The transformation fails at all points where rV_z equals zero or infinity.

References

[1] J.L. Lagrange, Memoire sur la theorie du mouvement des fluides, Nouv. Mem. Acad. Berlin, 1781.

[2] G.G. Stokes, On the steady motion of incompressible fluids, Cambridge Trans. vii, 1842.

[3] C.-S. Yih, Stream functions in three dimensional flows, La Houille Blanche 3 (1957) 445–450.

[4] J.H. Giese, Stream functions for three dimensional flows, J. Math. Phys. 30 (1951) 31–35.

[5] T.C. Benton, Example of the need for two stream functions in three dimensional flows, J. Math. Phys. 21 (3) (1962) 235–237.

[6] A. Breeze-Stringfellow and O.R. Burggraf, Computation of propeller nacelle interference flows using streamtube coordinates, in: K.N. Ghia and U. Ghia, eds., ASME Mini-Symposia on Advances in Grid Generation, University of Cincinnati, Cincinnati, OH (1985) 107–116.

[7] R. Ishii, Subsonic-supersonic flow in axially-symmetric nozzles, Trans. Japan Soc. Aero. Space Sci. 23 (59) (1980) 18–34.

[8] R. Ishii, Symmetric flow in axially-symmetric nozzles, Trans. Japan Soc. Aero. Space Sci. 23 (60) (1980) 67–78.

[9] C.E. Pearson, Use of streamline coordinates in the numerical solution of compressible flow problems, J. Comput. Phys. 42 (1981) 257–265.

[10] A.K. Singhal and D.B. Spalding, A 2D partially-parabolic procedure for axial-flow turbomachinery cascades, in: S.V. Patankar, A. Pollard, A.K. Singhal and S.P. Vanka, eds., Numerical Prediction of Flow, Heat Transfer, Turbulence and Combustion. Selected Works of Prof. D.B. Spalding (Pergamon Press, New York, 1983).

[11] H. Emmons, The numerical solution of compressible fluid flow problems, NACA TN 932, 1944.

[12] H. Emmons, The theoretical flow of a functionless, adiabatic, perfect gas inside of a two-dimensional hyperbolic nozzle, NACA TN 1003, 1946.

[13] H. Emmons, Flow of a compressible fluid past a symmetrical airfoil in a wind tunnel and in free air, NACA TN 1746, 1948.

[14] W.C. Chin and D.P. Rizzetta, Airfoil design in subcritical and supercritical flows, J. Appl. Mech. 46 (1979) 761–766.

[15] M. Hafez, Numerical solution of transonic full stream function equation in conservation form, Note 178, Flow Research Inc., Kent, WA, 1979.

[16] M. Hafez and D. Lovell, Numerical solution of transonic stream function equation, AIAA J. 21 (3) (1983) 327–335.

[17] A. Sherif and M. Hafez, Computation of three dimensional transonic flows using two stream functions, AIAA Paper 83-1948, 1983.

[18] H.L. Atkins and H.A. Hassan, A new stream function formulation for the Euler equations, AIAA Paper 83-1947, 1983.

[19] R. Courant, Different and Integral Calculus (Interscience, New York, 1947) Vol. II, Ch. III.

[20] N.E. Kochin, I.A. Kibel and N.V. Roze, Theoretical Hydrodynamics (Interscience, New York, 1964) 289–290.

[21] H. Lamb, Hydrodynamics (Dover Publications, New York, 6th edition, 1945) Art. 167.

[22] K. Karamcheti, Principles of Ideal-Fluid Aerodynamics (Wiley, New York, 1966) Section 4.9.

[23] W.R. Hawthorne, Engineering Aspects, in: R.J. Seeger and J.G. Temper, eds., Research Frontiers in Fluid Dynamics (Interscience, New York, 1965) Ch. 1.

[24] W.R. Hawthorne, N.A. Mitchell, J.E. McCune and C.S. Tan, Nonaxisymmetric flow through annular actuator disks: Inlet distortion problem, J. Engrg. Power 100 (1978) 604–617.

[25] S.O. Buneman, Ideal gasdynamics in Hamiltonian form with benefit for numerical schemes, Phys. Fluids 23 (1980) 1716–1717.

[26] C. Lacor and C. Hirsch, Nonviscous three-dimensional rotational flow calculations in blade passages, in: H. Viviand, ed., Proceedings of the Fourth GAMM Conference on Numerical Methods in Fluid Mechanics (Vieweg, Braunschweig, 1982) 150–160.

[27] W.R. Hawthorne, C. Wang, C.S. Tan and J.E. McCune, Theory of blade design for large deflections: Part I, Two-dimensional cascade, J. Engrg. Power 106 (1984) 346–365.